Untargeted FTICR-MS Based Plasma Metabolomic Analysis and Translation to Type 2 Diabetes

Yanlong Zhu[1], Benjamin Wancewicz[1], Michael Schaid[1], Kent Wenger[1], Yutong Jin[1], Heino M. Heyman[2], Christopher J. Thompson[2], Aiko Barsch[3], Allan Brasier[1], Michelle Kimple[1], Ying Ge[1]

[1]University of Wisconsin-Madison, Madison, WI 53705, [2]Bruker Daltonics Inc., Billerica, MA 01821, [3]Bruker Daltonik GmbH, Bremen, Germany 28359

Overview

- We introduced a high-throughput, highly reproducible FTICR-MS based platform for plasma metabolomics.
- Rapid untargeted plasma metabolic phenotyping identifies both Type 2 diabetes fingerprint and specific metabolic changes.
- Mouse plasma samples were used for development of FTICR-MS based platform for metabolomics.
- Plasma samples from diabetes-susceptible human were analyzed via developed FTICR-MS based platform.

Introduction

Type 2 diabetes (T2D) is an extremely prevalent metabolic disorder that negatively affects the health of hundreds of millions of people worldwide. A number of circulating metabolites have been positively associated with T2D status in both pre-clinical models and human populations. However, it is unclear whether the observed metabolic changes are a consequence of high glucose levels and therefore of the T2D or if the metabolic changes are causative and lead to the development of T2D. Here, we report a high-throughput ultra-high resolution magnetic resonance mass spectrometry (MRMS) based platform for plasma metabolite fingerprinting, which provides broad metabolic profiles in minutes. This new platform was used as a first-pass tool to investigate the fundamental changes in metabolism associated with T2D.

Methods

FTICR-MS Based Plasma Metabolomic Analysis

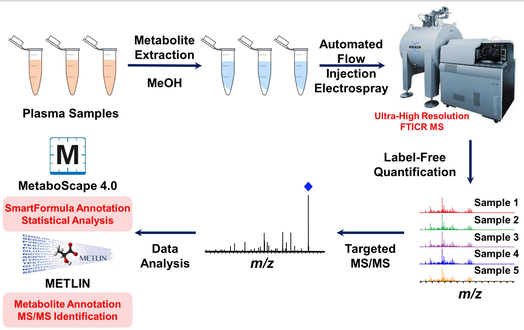

Figure 1. Workflow of FTICR-MS based platform for plasma metabolomics. Metabolite extracts were directly injected into FTICR-MS without LC separation. MS: Bruker solariX 12T FTICR mass spectrometer.

Sample Information

1. Mouse Plasma Samples:
Obese mice with Purina diet and severely insulin resistant were used for development of FTICR-MS based platform for plasma metabolomics.

2. Human Plasma Samples:
Control (n=14); T2D-DL (n=6); T2D-M (n=9)
Diet/Lifestyle; Metformin

Data Analysis Parameters

MetaboScape 4.0 Bucket list: T-ReX 2D Algorithm
mzDelta: 0.5 mDa
Max. Charge: 3
Intensity Threshold: 0
Minimum # Features for Results: 5
Positive Mode: +H, +NH_4, +Na, +H-H_2O
Negative Mode: -H, +Cl

MetaboScape 4.0 SmartFormula Annotation:
Mass Accuracy: Δm/z < 2 ppm; Δm/z < 5 ppm
mSigma* (Δm/z < 2 ppm): < 20; < 50

*Isotopic pattern fit score

METLIN Annotation:
Δm/z < 2 ppm

Results and Discussion

FTICR-MS Based Platform for Metabolomics

1. High Reproducibility

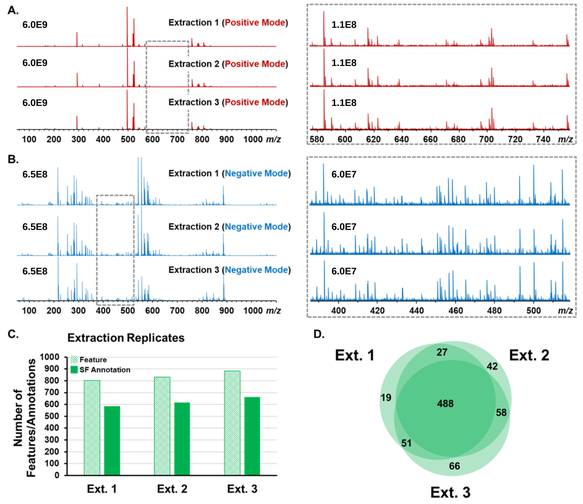

Figure 2. A. Mass spectra and zoomed-in mass spectra of 3 extraction replicates of mouse plasma sample in positive mode. **B.** Mass spectra and zoomed-in mass spectra of 3 extraction replicates of mouse plasma sample in negative mode. **C.** The numbers of features after blank reduction and SF annotations of 3 extraction replicates. **D.** Venn diagram of SF annotations from 3 extraction replicates (3 injection replicates in each extraction).

2. Ultra-High Resolution FTICR MS

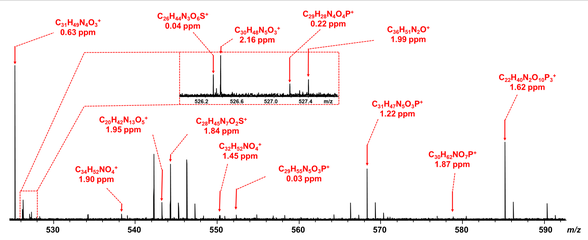

Figure 3. Representative ultra-high resolution FTICR mass spectrum. 13 unique SmartFormula annotations are identified in the 70 m/z window.

3. MS/MS Capability for Targeted Metabolite Identification

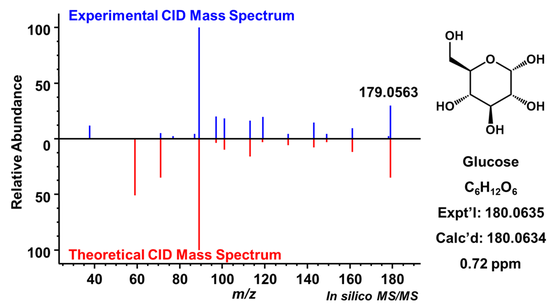

Figure 4. MS/MS analysis of metabolite at 179.0563 m/z. The experimental CID mass spectrum is compared with the theoretical CID mass spectrum of glucose.

Human Plasma Metabolomic Analysis

1. Overview of 3 Human Groups

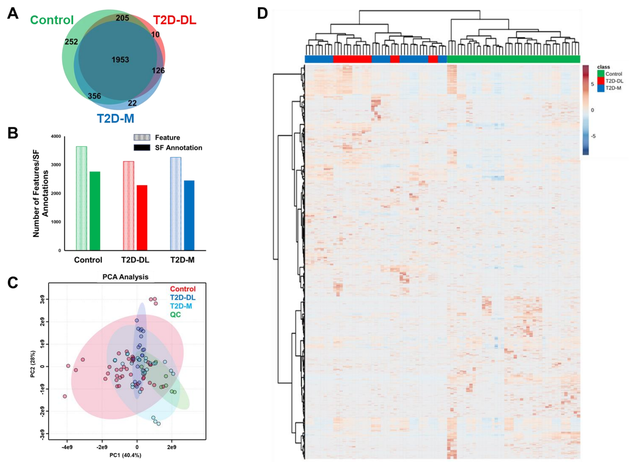

Figure 5. A. Venn diagram of SF annotations from Control, T2D-DL, and T2D-M human plasma samples. **B.** The numbers of features (light shading) and SmartFormula annotations (solid shading) from MetaboScape 4.0 (Δm < 5 ppm) of 3 human groups. **C.** Principal component analysis (PCA) of the 3 human groups and quality control group (QC). **D.** Heat map represents all features in 3 groups.

2. Control Group vs. T2D-DL Group

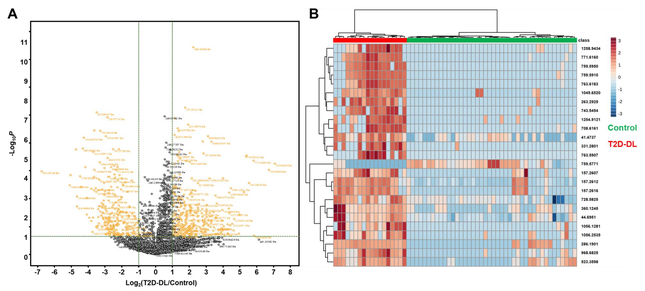

Figure 6. A. Volcano plot of Control vs. T2D-DL groups. 921 blank-reduced features show statistically significant differences (p(FDR) < 0.05). **B.** Heat map represents top 25 significant features from t-test analysis of Control vs. T2D-DL.

3. Control Group vs. T2D-M Group

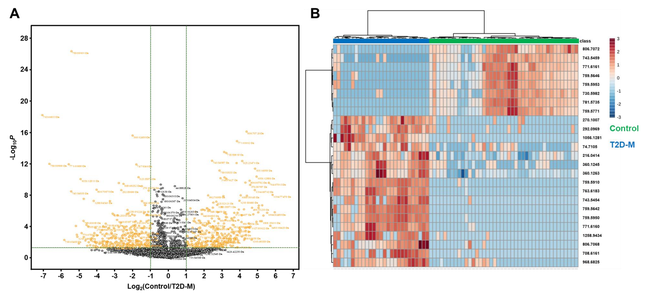

Figure 7. A. Volcano plot of Control vs. T2D-M groups. 952 blank-reduced features show statistically significant differences (p(FDR) < 0.05). **B.** Heat map represents top 25 significant features from t-test analysis of Control vs. T2D-M.

4. T2D-DL Group vs. T2D-M Group

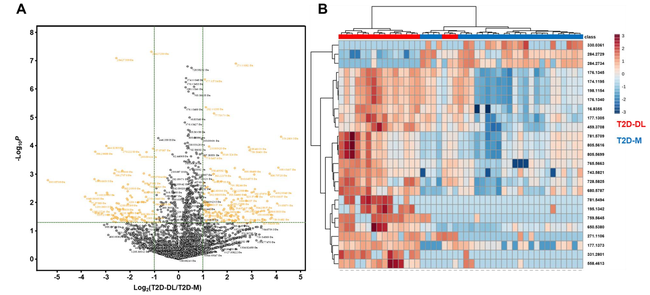

Figure 8. A. Volcano plot of T2D-DL vs. T2D-M groups. 95 blank-reduced features show statistically significant differences (p(FDR) < 0.05). **B.** Heat map represents top 25 significant features from t-test analysis of T2D-DL vs. T2D-M groups.

5. Chemical Similarity Enrichment and Pathway Analysis

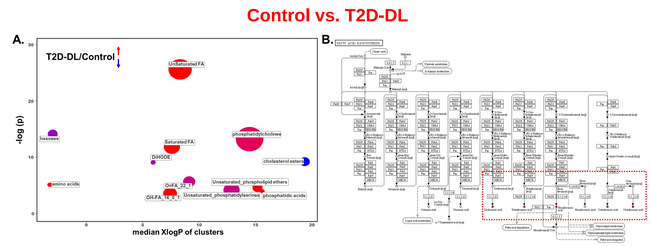

Figure 9. A. Chemical similarity enrichment analysis of Control vs. T2D-DL groups. The node sizes represent the total number of metabolites in each cluster set. The node color scale shows the proportion of increased (red) and decreased (blue) metabolites. **B.** Fatty acid biosynthesis pathway of Control vs. T2D-DL groups. All metabolites identified in this pathway increase in T2D-DL group. Pathway analysis was performed using KEGG Mapper.

Conclusions

- We introduced an integrated high-throughput FTICR-MS based platform for plasma metabolomic analysis.
- High injection and extraction reproducibilities were achieved.
- Thousands metabolic features were reproducibly detected and annotated in each human plasma group.
- MS/MS capability increases the confidence of targeted metabolite identification.
- This platform revealed significant metabolic changes in plasma from control vs. T2D human subjects, suggesting its place as a future tool for personalized T2D therapy.

Acknowledgements

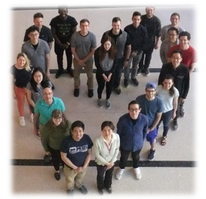

The authors would like to acknowledge the NIH Grants, R01HL096971, R01HL109810, R01GM125085, R01GM117058, S10 OD018475, R01DK102598, and CTSA grant 1UL1TR002373. The authors also thank the instrumental and technical support of Bruker Daltonics, and group members of the Dr. Ying Ge's research group.